Atmospheric effects on FPAs in IRSTs

Piet Schwering

TNO Physics and Electronics Laboratory
P.O. Box 96864, NL–2509 JG The Hague, The Netherlands
E-mail: Schwering@fel.tno.nl

ABSTRACT

In 1993 and 1994 TNO-FEL participated in the execution of experiments over the North Sea in order to derive the infrared atmospheric scintillation and beam deformation process. In 1993 the NATO MAPTIP trial allowed us to observe an infrared point source from a platform at sea with a 10 micron FLIR, at various ranges (0.5-5 NM) and in various directions. In 1994 an infrared source was used at fixed distances on a platform at sea, with heights at the platform ranging between 1.5 and 7 m above the sea level. Some additional sources, at different height levels, were installed later in the experiment. The receiver system was placed at 18 km on a pier near the Dutch coast. Recordings took place with the receiver at two heights, 40 and 15 m above the average sea level. A single recording consisted of 10 seconds of measurements at 25 Hz with a 64x64 Cincinnati IRC-64A camera in the 3-5 μm band. Also data in the 10 μm band is available. We have also executed experiments with a source on a boat sailing out from close by to the optical horizon. Examples of these recordings are presented. The data were analyzed for scintillation effects, atmospheric APSF effects and refraction effects. These data are compared to the atmospheric conditions that were recorded simultaneously, in order to model the infrared scintillation effects with meteorological conditions. In the paper we describe the analysis, results on the atmospheric effects with meteorological condition and with range. Results of these comparisons are also shown. We discuss the effects that these results have on the performance of IRSTs, and how improvements can be made to the IRST based on these results.

1. INTRODUCTION

For the detection of low observable infrared targets near the sea surface at large distances it is of great importance to optimize the signal to noise ratio. With the use of two-dimensional FPA infrared detectors placed in large optics, we have the opportunity to improve the signal to noise ratio by a large factor. The use of staring FPA detectors have some more favorable effects. Their high frame update rate makes it possible to improve tracking capabilities. The best choice of processing is possibly a mixture between frame-to-frame integration to improve the signal to noise ratio, and exploit the better tracking capabilities.

In this paper we present our research in the field of maritime atmospheric effects on infrared systems. Our aim is to investigate the atmospheric limitations for these systems, especially for their use with targets near the sea surface at large distances. An important fact is the effect of turbulence on the infrared imagery. Turbulence leads to scintillation in the imagery, which can be identified by fluctuations (in intensity and in shape) of point sources. In the case of detection, it is important to know the amount of fluctuation that can be expected from scintillation, and during which meteorological circumstances we may expect most scintillation.

0-8194-1911-7/95/$6.00

This paper deals mainly with the atmospheric scintillation effects that are recorded over large distances over sea.

Scintillation over sea is expected during several different meteorological situations. The parameters that are of most influence are the air to sea temperature difference (ASTD), the aerosol content (depending on wind speed and wind direction), relative humidity and air temperature. Therefore we expect different scintillation results to occur with the various distances. Changes in these parameters create small refractive index effects in the air. We aimed to record scintillation in the experiments for a wide range of meteorological parameters and for many distances, in order to build up some quantitative maritime statistics concerning scintillation with respect to distance and the meteorological situation. This description determines the experimental setup that was chosen. Land based Point Spread Function (PSF) measurements and a theoretical description was given by Sadot *et al.* (1994)[1] and references therein. Scintillation over sea is known to occur at visual wavelengths. At infrared wavelengths similar scintillation effects are expected.

2. OBSERVATIONS AND DATA REDUCTION

The main requirement of an experimental setup for the study of maritime scintillation is that the experiments should be executed over sea, in order to minimize the direct influence of land and its turbulence effects. The setup of the experiment requires an infrared emitter and receiver, at two different locations. We have participated in three experiments in 1993 and in 1994.

2.1. NATO MAPTIP trial

During the 1993 NATO AC/243 Marine Aerosol Properties and Thermal Imager Performance trial (MAPTIP, de Leeuw *et al.*, 1994[2]) we have used helicopter flights during which a tethered point source was lowered to approximately 10 m above the sea level. The MAPTIP trial took place from October 11 until November 5 of 1993. The infrared source, also called the Helicopter Glow Source, designed and developed at TNO-FEL, is calibrated at the applied voltage of 27 Volt to be 13.2 Watt/sr in the 3-5 μm band and 5.5 Watt/sr in the 8-12 μm band. The calibration of the source was performed with the DuDa imager[3]. The heat up time of the source was about 30 minutes. The observer was positioned at a height of about 15 m above the mean sea level at the Meetpost Noordwijk platform, hereafter MPN (52 °16 ′25.9 ″N, 04 °17 ′45.8 ″), which is located at about 10 km from the coast of Noordwijk (The Netherlands), in the North Sea. This receiver, a USFA UA-92 8-10.7 μm FLIR with 0.17 mrad IFOV, was used to record data from the source on a Umatic recorder in an analog way. The source has a size of about 40 cm and can be considered to be a point source for the FLIR from distances larger than 2.3 km. The UA-92 FLIR makes use of a CMT Sprite detector, and creates CCIR images at a 25 Hz frame rate by horizontal and vertical scanning. Due to the scanning mechanism of this imager we have a good sampling on the image lines. These data were later digitized in 8 bit via an DT-2851 frame grabber, and also with a Matrox Magic frame grabber. We have also recorded a limited number of frames directly in digital form but with the aim of analyzing scintillation the analog tape data was of greater use. The DT-2851 frame grabber digitizes a 512x512x8 bit image at a rate of 2.5 Hz. The analysis typically used data of 50 frames, hence over a period of 20 seconds. The latter frame grabber has a higher sampling rate and therefore reduces possible under-sampling effects. This grabber was used to sample 752 pixels on a line for 100 frames at full frame rate of 25 Hz (hence 4 seconds of data). These latter data were used to compare the results of the first grabber for under-sampling errors. The digital data was analyzed with the sequence analysis toolkit ANALSEQ 1.55 developed at TNO-FEL.

The helicopter was positioned at various distances from the MPN platform and also at different directions. Some of the positions were in the direction of the coastal background while others were in the direction of the

sea (also sun glints). From these data an analysis of the signal and its variations with distance is possible. In this way, during MAPTIP, we have created transmission and scintillation links at sea over various path distances ranging from 0.5 up to 20 Nautical Mile. For the 10 micron FLIR with this sensitivity, data beyond a range of 5 NM is not useful for quantitative analysis due to the low signal-to-noise ratio.

2.2. Coast-MPN experiment

In 1994 TNO-FEL has set up an experiment in which a calibrated infrared source was placed at a large distance from the observer on the same MPN platform in the North sea. The emitter source is an glowing emitter heated by a power current of maximum 60 Volt at 8.4 Amperes. The heat up time is then about 10 minutes. A NiCr-Ni thermocouple registers the temperature of the ceramic element. The source can be used at an intermediate temperature as well. This glowing element, a piece of ceramic, is placed in the focus of a parabolic mirror with an outer diameter of 75 cm and an inner obscuration of 18 cm diameter. The element reaches a temperature of 760 degrees Celsius and has an emission coefficient of about 60 %. To prevent the source from corroding a foil with 80 % transmission was used in front of the source. The total radiance emitted by the source is about 850 (3-5 μm) and 340 (8-14 μm) Watt/sr. The source was calibrated in the laboratory by comparing with a calibrated 900 K source, and recording the signals with the DuDa imager[3]. Due to the short focal length compared to the length of the ceramic material, the beam width is about 8 degrees. The source is mounted on a lift to move it from 1 m up to 7 m above the sea level. The source is well isolated from the platform itself to avoid warming up of the platform construction. When the source is not used, it is kept is a cage for protection. During a later stage of the measurements, a 60 cm diameter diaphragm was installed before the source to reduce the signal.

At MPN, owned and maintained by the Netherlands Ministry of Public Works, standard meteorological data is gathered as a standard procedure. These data include tidal motion at MPN as well as on other locations near the coast. Beside these standard data TNO-FEL also records additional meteorological information including visibility, solar radiation and a relative humidity profile with heights above 4 m. These latter data are stored on a personal computer at MPN.

The receiver is located at the pier of Scheveningen (52°07'04.6"N, 04°16'49.0"E) at 40 m above sea level. Later in the experiment the receiver was lowered to a height of 15 m. The measurement location at the pier is about 200 m away from the beach. We make use of the Experimental Thermal Infrared System II (ETIS-II), which is a parabolic mirror system with a 30 cm aperture with a 1 m focal length. The ETIS-II system is described by de Jong (1977)[4]. As detectors we use a 2.3-4.7 μm Cincinnati IRC-64A (64x64 staring FPA) and a 8-14 μm Graseby (28 element staggered 1D array) detector. In this paper we are only using the 4 μm Cincinnati data. The IRC-64A is connected to a personal computer with a IRC-DCB2 board installed to record the 12 bit data digitally for 10 seconds (all 25 frames per second). The resolution of this instrument is 0.05 mrad (determined by the square pitch) with 0.028 mrad sensitive square pixel elements (30 % fill factor). The detector NETD is about 0.02 degrees at 21 degrees Celsius. These data are recorded on the computer hard disk and transported to the TNO-FEL laboratory for off-line analysis. A preliminary analysis of all the imagery is done directly afterwards. At the location of the pier we also control the position and the intensity of the source and it records the meteorological data that is gathered at MPN. This remote control goes via a radio communication link.

In this case we have created a scintillation link over sea over a path of 9.3 Nautical Mile. For a similar path transmission measurements were executed in 1978[5]. The transmission measurements showed at that time that the transmission is quite good in general over this path (20-50 % in the 3-5 and 8-12 μm bands). The size of the source (0.75 m) is smaller than a resolution element at the distance of 17.2 km (0.9 m at 4 μm). We therefore expect the source to be a perfect point source, smoothed by atmospheric effects to a

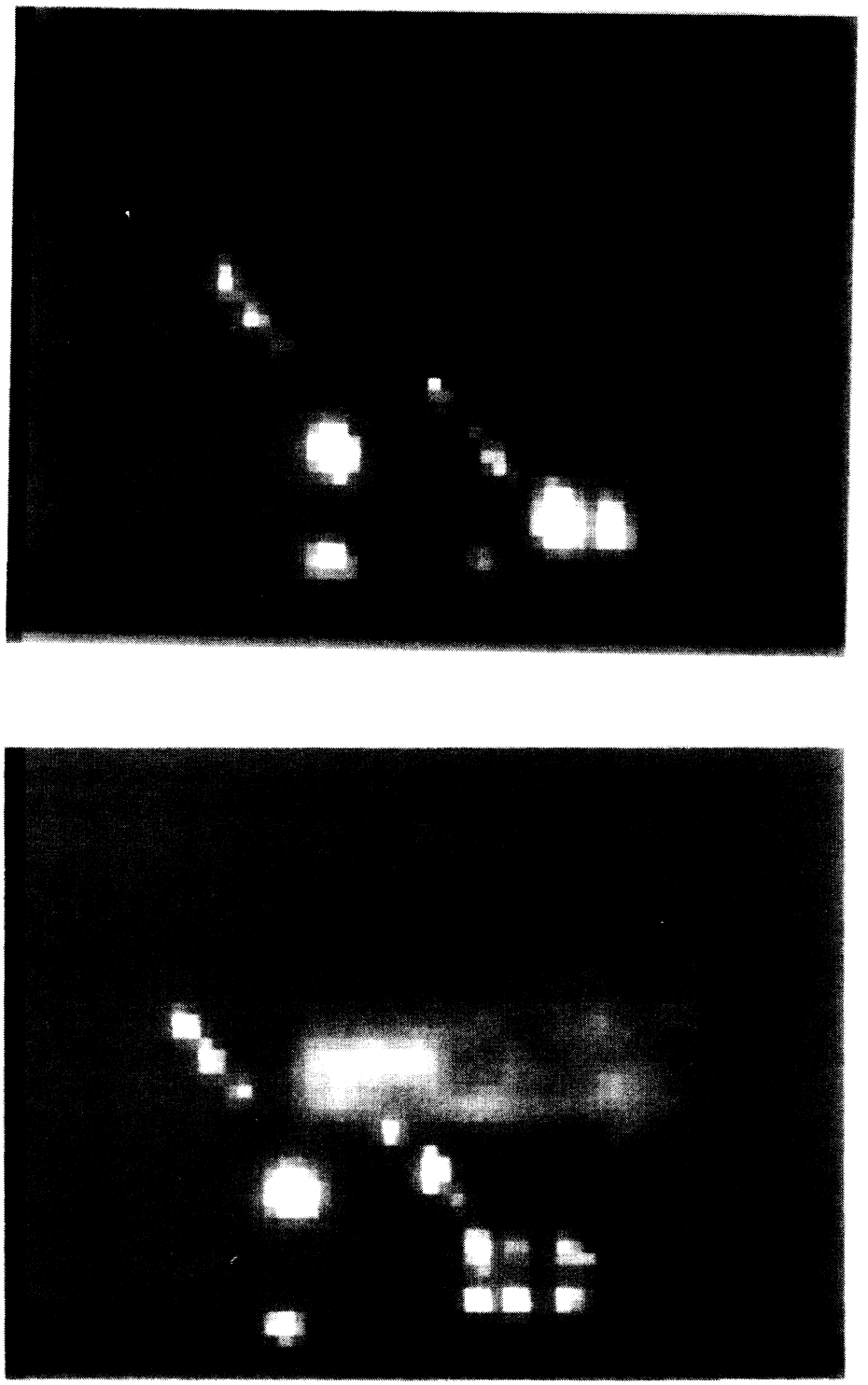

Figure 1: 4 μm Cincinnati IRC-64A images with the ETIS-II telescope of MPN with the infrared source and the nine lamps. Upper image: 30 August 1994; Lower image: 23 September 1994.

more extended object. For the system at 40 m height the horizon will be at 23 km. A path that intersects the sea at 17 km is 0.005 degrees below the horizon, hence the (unrefracted) line-of-sight has the lowest height near the target.

Point Spread Function (PSF) recordings were made in the spring, summer and fall of 1994. During the first months of recordings, measurement recordings are typically done at all stops of the lift above sea level. During the later stages only the higher source levels were used for recording. At each of the stops data are gathered for the Cincinnati IRC-64A (4 μm), for 10 seconds of 64x64 12 bit frames at 25 Hz (2.0 Mbyte of data), *i.e.* 250 consecutive frames. The signal of the source was lowered in a number of occasions by placing diaphragms in the ETIS-II system in front of the parabolic mirror.

2.3. Refraction experiment

In the summer of 1994, under contract with the Defence Research Establishment Valcartier, a total of nine lamps were placed at different heights at MPN (from a height of 4.5 up to 18 m diagonally). The goal of this study was to investigate refraction effects at visible wavelengths. Figure 1 shows two grey scale images during the 1994 experiment of a Cincinnati IRC-64A 3-5 μm image made with the ETIS-II telescope from the infrared source and the nine visible light lamps. The infrared source was the main subject of study, while the visible light lamps (500 Watt lamps for a building site) were used in the additional project concerning refraction. In the images, whiter grey scales represent higher apparent temperatures. During the upper image recording the pressure was 1016 hPa, relative humidity of 87 %, ASTD of -3.4 °C, wind speed 3.8 m/s. We observe a cold sea and a somewhat warmer sky background. Note that these apparent temperatures are not the same as the measured true temperatures due to reflection at the sea surface at gazing angles. The presence of mirages agrees with the large negative ASTD. The horizon is not very sharp. The MPN platform is also seen as cold against the sky background. The nine visible lights are placed diagonally from upper left to lower right. The lowest two lamps (at the same altitude at the right) are on the optical horizon and due to an atmospheric lens effect the brightness is about a factor of four to five larger than for a normal unrefracted lamp. The second lowest lamp is seen as normal mirage in the sea as well. The infrared source is seen as the bright source at the left with a mirage in the sea. The lower image of figure 1, recorded while the ASTD equals -2.0 °C, shows similar mirage effects for all the lower lamps, and no lens effect is present. The platform seems warm against a cool sky background.

These data obtained in the refraction experiment, in principle give us scintillation data over various heights above the sea level from 4.5 up to 18 m at a distance of 18 km. Additionally, data were recorded with a ship supplied with three similar lamps. From these latter ship measurements we obtained information of scintillation with range.

3. THEORETICAL TURBULENCE MODEL

Infrared atmospheric turbulence effects in the surface layer can be estimated from the refractive index structure function parameter C_n^2 that is closely related to turbulent fluxes of sensible heat and water vapor. Using standard meteorological observations in combination with generally accepted micro-meteorological models, these fluxes can be calculated (see *e.g.* Davidson *et al.* 1981)[6]. In addition, vertical profiles for wind, temperature, humidity and thus for the refractive index of air can be estimated to predict refractivity effects. The TNO-FEL turbulence model will be described in full details in an upcoming publication (Kunz, 1995). Examples of these model calculations, showing the refractive index structure constant as a function of ASTD, of wind speed and of height, have been presented in an earlier paper[7].

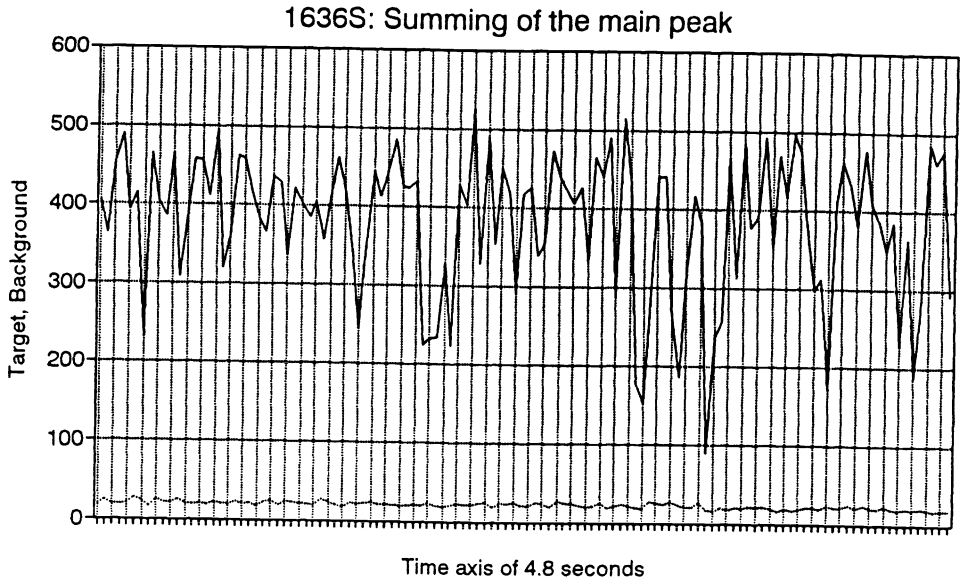

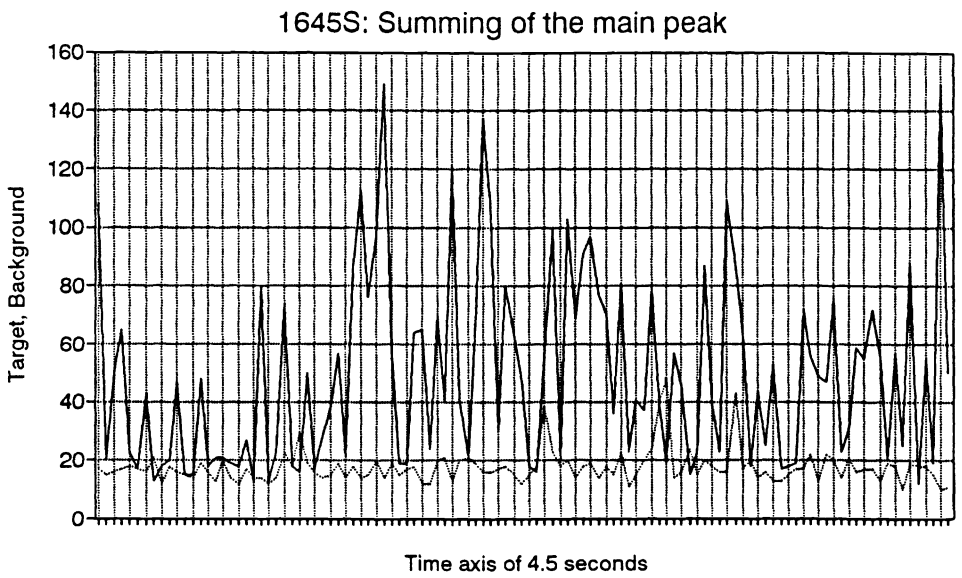

Figure 2: Time series of analysis of the Helicopter Glow Source data of 26 October 1993 at 16:36 CEST (2.5 NM above) and at 16:45 (5.0 NM below).

4. DATA ANALYSIS

In this section we analyze the scintillation effects with range from the MAPTIP data and with meteo parameter from the longer term Coast-MPN experiment.

4.1. Scintillation effects with range

From the MAPTIP data of the Helicopter Glow Source we have selected data from October 26, 27, 28 and 29. Data with the source at distances between 0.5 and 5 NM were digitized with the DT-2851 frame grabber and analyzed via the programme ANALSEQ 1.55. This algorithm searches in a box surrounding the position of the glow source in the image for the true peak, and it integrates the signal by summing the peak for all image pixel values in this single peak that are beyond the local average background increased by two times the local RMS value. These local average background and RMS are calculated in a two pixel wide surrounding box that excludes the search box. The search box is pin-pointed by the operator by hand. This algorithm is more stable against noise than a simpler one, as was shown by applying the same algorithm on a piece of empty background. For images with the source close-by a similar value was obtained as by simple integration of a block around the source, compared to the local background. For small and dim sources however the latter algorithm shows large fluctuations due to the varying (or noisy) background. The results from the first algorithm are much stabler at longer ranges. We therefor use the data gathered by the first algorithm. Table 1 gives the data obtained in this way. For the various dates and times, at various ranges the table presents the source's integrated intensity with its fluctuation, the empty background integrated intensity and the fluctuation, together with the ratio of RMS in the sea compared to the empty sky.

The results from the analysis in Table 1 are as follows. At increasing distances we observe a decreasing source signal and an increasing relative fluctuation. The decrease of source signal at short ranges (1 NM) is less than expected for point sources. One of the reasons for this is that we look at contrast values with respect to a varying background (coastal, sea or sky), hence the background changes with the range parameter. Even at long ranges, 5 NM, the source's image still represented about six pixels. Hence we conclude that there is no under-sampling present in the images. From data digitized with the Matrox frame grabber, with a higher sampling rate, similar fluctuations were observed at long ranges. We observe the source signal at 5 NM even a factor of three beyond the empty background peaks. At short ranges (1 NM) fluctuations occur of about 10 %. At 2.5-3 NM typical fluctuation values occur of 20-30 %. At 5 NM fluctuations of 60-70 % are about similar to the fluctuations that occur in the empty background, but on average still somewhat lower. Hence we observe an increasing fluctuation of the signal with distance. This is what is expected from the increasing amount of turbulence with the longer path.

Data recorded on October 26 at 2.5 and 5.0 NM with the UA-92 FLIR was digitized frame-by-frame with the Matrox Magic frame grabber for resp. 4.8 (120 frames) and 4.5 sec (113 frames). The integrated intensities determined via the method described above are recorded in time series in figure 2. The bolder curve shows the Glow Source data while the thinner curve shows the results for a piece of empty background. Note that at the larger range the fluctuations become severe and even make the source's signal disappear sometimes. It then becomes impossible to distinguish the source from the empty background. This behavior is also observed in the infrared images.

Figure 3 presents two images of the source at 5 NM. The upper image is a Laplace filtered section of a single image frame. Note that we observe the helicopter as a bright source, but the Glow Source is not observed. The lower image is a Laplace filtered image section of the average of the 113 frames. Note that both the helicopter and the Glow Source are observed. Also the horizon is present in this image. At the right of the images we present vertical cross-cuts through the image column that intersects the helicopter and the

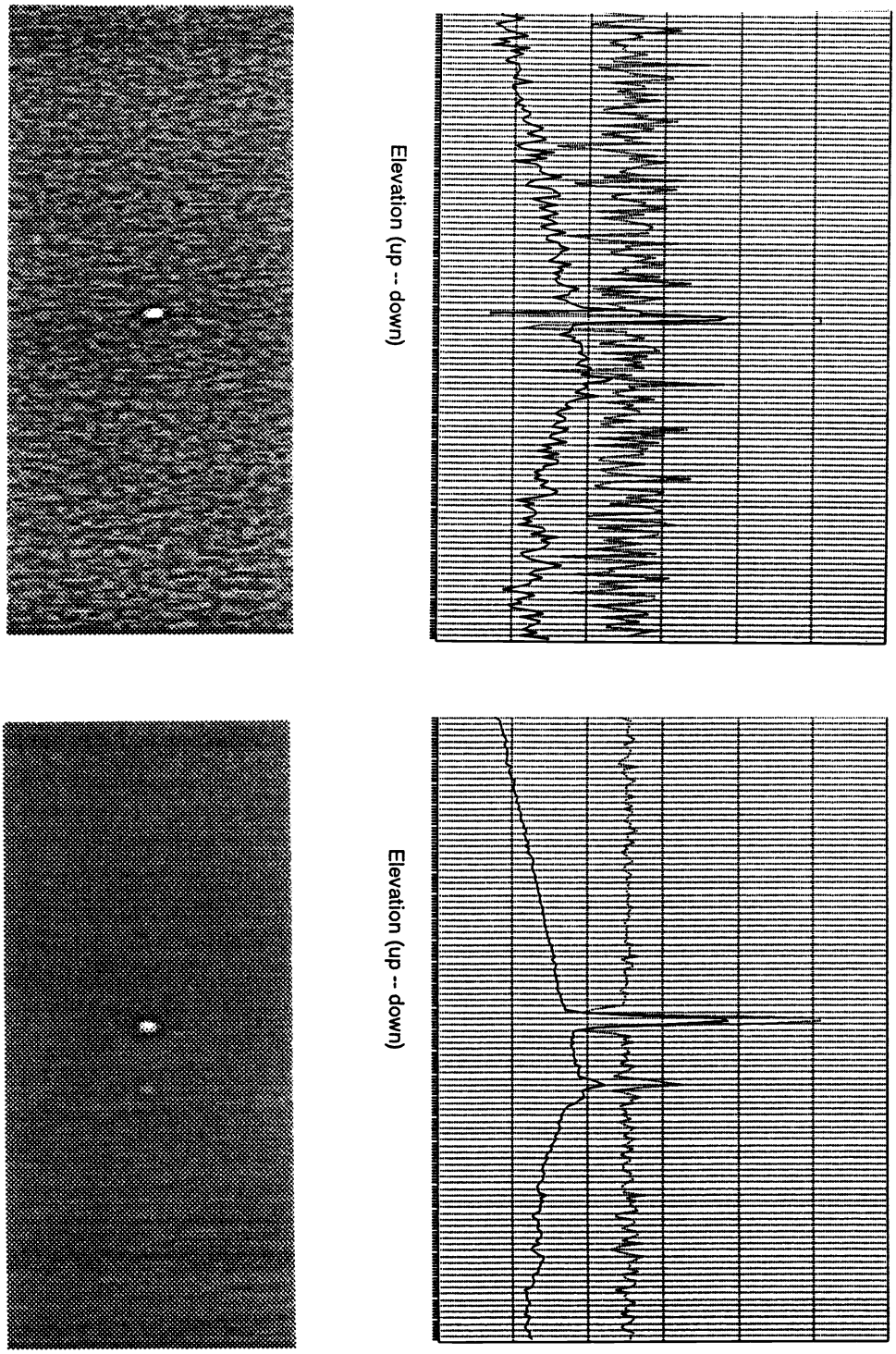

Figure 3: Imagery at October 26 at 5 NM. The upper image is for a Laplace filtered single frame, and the lower image for the Laplace filtered averaged frame. At the right vertical cross-cuts through the original and Laplace filtered images are presented.

source, both through the unfiltered image and through the Laplace filtered image at 5 NM. The unfiltered signal has the slope in the sky while the filtered image has a flat background. Also in these representations, we are able to observe the Glow Source only in the averaged imagery. Note also that the noise has been canceled out by a large amount.

Table 1: Helicopter Glow Source data recorded during MAPTIP.

Date	Time (GMT)	Range (NM)	Source (arb)	Fluct. (%)	Backgr. (arb)	Fluct. (%)	Sea/Air RMS
26-10-93	15:29:30	0.5	4261.3	0.07	54.7	0.75	1.25
	15:24:02	1.0	1958.7	0.05	23.6	0.90	1.22
	15:37:30	2.5	380.1	0.10	15.1	0.80	1.27
	15:15:38	3.0	146.8	0.22	17.7	0.70	1.05
	15:44:35	5.0	49.6	0.46	15.1	0.62	1.33
	15:09:18	5.3	42.8	0.69	20.1	0.66	1.09
27-10-93	15:28:20	1.0	1306.3	0.09	27.9	0.86	1.00
	15:38:25	2.5	363.5	0.43	20.8	0.72	1.07
	15:20:15	3.0	215.3	0.28	110.1	0.72	1.06
	15:41:50	5.0	41.5	0.62	16.4	0.65	1.14
28-10-93	15:33:30	1.0	1579.1	0.13	24.7	0.77	1.95
	15:43:59	2.5	447.1	0.17	14.1	0.55	2.80
	15:23:21	3.0	66.8	0.18	30.9	0.46	2.85
	15:51:45	5.0	50.2	0.61	14.7	0.82	2.29
29-10-93	15:09:24	0.1	8700.0	0.09	59.5	0.68	2.48
	15:00:18	1.0	2135.6	0.10	18.4	0.61	2.63
	15:18:05	2.5	412.8	0.15	15.8	0.86	2.57
	14:56:25	3.0	135.5	0.57	17.2	0.98	3.64
	15:28:36	5.0	52.6	0.70	11.6	0.79	0.43

4.2. Scintillation effects with meteorological condition

Images of a MPN infrared point source of the 1994 trial were analyzed with respect to the background level for maximum intensity (contrast), volume (integrated contrast over the point source), equivalent diameter, ellipticity and position of the point source image. In addition, the skewness and the kurtosis of the point source image were determined to quantify distortion and spatial distribution of the intensity over the image plane. The results were used to define scintillation, blur, image dancing and distortion of the imaged spot. For the analysis of the volumes of the point source images, we applied a 10 % contrast level criteria to identify the pixels being part of the imaged point source. Of course, this might result in a slight underestimate of the volume but lower level detection criteria on the other hand, have shown to be sensitive to overestimating the volume due to integration of the background intensity. We have applied several other segmentation techniques for testing purposes, some based on other (relative or absolute) threshold levels others based on spatially

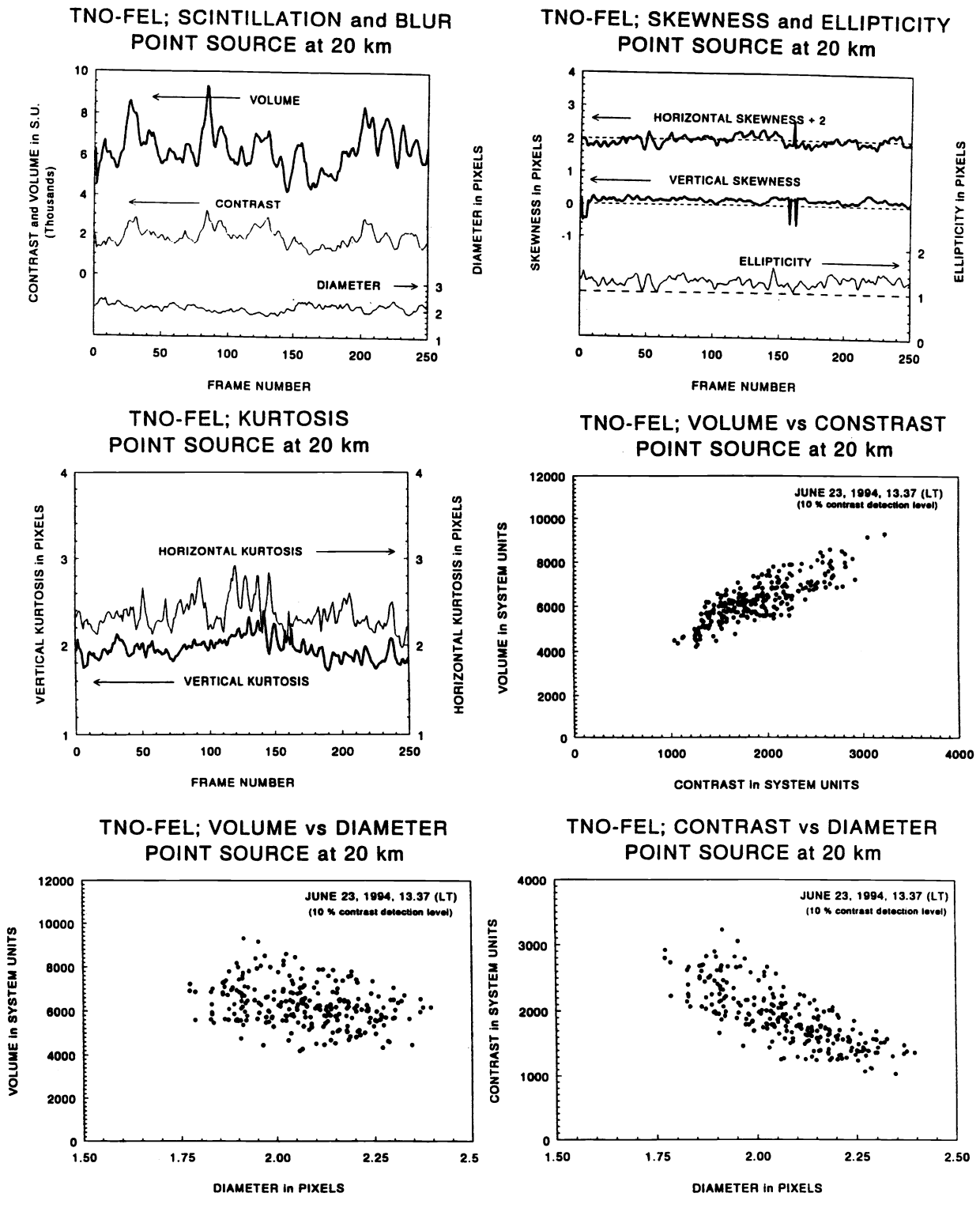

Figure 4: Time series and scatter diagrams of the analysis of the infrared source data of 23 June 13:37 CEST (frame rate 25 Hz).

fixed or growing areas.

The ratio of the volume and the peak intensity has been used as a measure for the size of the spot in the image plane. Thus volume and peak intensity are two independently determined quantities. Comparison of the spot size from laboratory measurements in combination with the temporal variation provides a measure of the blur. The stability of the coordinates of the centroids of the imaged spot is a measure for the image dancing whereas the variation in volume and maximum intensity are a measure for the scintillation.

As an example, we present some results derived from a set of 250 images recorded during an unstable condition on 23 June 1994 at 13^h:07^m CEST, with good visibility (about 40 km), ASTD of -2.0 °C, relative humidity of 60 % and a wind speed of 1.3 m/s, all measured at a height of 15 m. Figure 4 presents time series derived for the quantities determining the scintillation and blur. From the contrast and volume time series we note that there are relatively slow typical variations (0.2 sec.), much slower than the frame rate (25 Hz). This could be the result of a limited size source. Of course we observe all kinds of frequencies, also at high scales as well as low scales. The spectral behavior of the integrated intensity of the infrared point source shows a $\nu^{-5/3}$ power law. This corresponds to the frequency distribution of Kolmogorov turbulence theory. The calculated fluctuation in the signal of this example is 60 % (over 9 NM).

From scatter diagrams (figure 4) we have observed that the integrated intensity over the point source varies by about a factor of two and is not related to the diameter of the spot size. We have also observed that the diameter of the spot size varies from about 1.7 pixels to about 2.4 pixels. Laboratory tests indicated a minimum spot size of about 1.6 pixels. Apparently, due to atmospheric effects, the diameter of the imaged point source increased from about 5 % to about 50 %. Although there is no correlation between the point integrated intensity and the diameter of the imaged spot, the maximum intensity is positively correlated with the volume (integrated intensity) and negatively with the diameter of the imaged spot. Because volume and contrast are positively correlated, it is concluded that this effect is caused by transmission losses (the real part of the propagation coefficient) over the path of observation. Apparently, the diameter is better correlated with contrast than with volume. This is expected from blurring effects, where the integrated intensity might be kept constant while the peak gets sharper and larger or when it gets broader and lower. Of course both volume and peak can still vary in time due to transmission losses by passing turbulence. For sea winds, the observed scintillation and blurring corresponds well with the expected model behavior[7].

5. DISCUSSION

We have observed scintillation effects both in the FPA data and in the scanner data. Also the relative amount of fluctuations in the FPA and scanner data are similar. This means that the effect of the under-sampling in the FPA by the filling factor less than one is not the dominating factor in the FPA.

From the fact that the fluctuations increase with distance we expect targets at long ranges to have large signal fluctuations. The amount of fluctuation at these long ranges is about equal to the background fluctuation. The increase of scintillation with distance is expected from the physical models.

The fact that signal fluctuations occur at frequencies of 5 Hz for bright sources, does not necessarily mean that this is also the case for dimmer sources. We may expect larger frequencies for dimmer sources due to the possibility that the lower frequencies may depend on a stronger target signal.

For present day revolving IRST systems with frame rates of 1-2 Hz these fluctuation frequencies of 5 Hz are too high and under-sampling in time of these scintillation effects clearly occur. This means that the signals of the source at long ranges will be uncorrelated in two or more frames. The best we can do in these cases is to average frames or to correlate detections in consecutive frames with some kind of association

process. When we apply higher frame rates, such as in a 25 Hz staring system, we would be able to apply algorithms that would predict more accurately the target signal based on the observed temporal correlation. Therefore the tracking of targets with these systems would benefit by applying a filter adjusted to the filter output of the previous frame.

6. CONCLUSIONS

In this paper we have presented our preliminary analysis of the TNO-FEL atmospheric Point Spread Function studies. We have described the measurement setup of three trials of 1993-1994 and the observations as well as the preliminary data reduction. We have observed severe scintillation with distance, both with FPAs as well as with scanning devices. We have also observed an increase of scintillation with distance. Fluctuation levels of 50-60 % at 5 NM is quite normal. The results are discussed in terms of applications in future IRSTs with high frame rates.

7. ACKNOWLEDGMENTS

I would like to thank the Van der Valk company, owner of the pier in Scheveningen, and particularly Mr. H. Luiten, for allowing these measurements to take place. Thanks are also owed to the Netherlands Ministry of Public Works and in particular Mr. G. Goossens and Mr. J. v.d. Horn for supporting the work at the MPN platform. I acknowledge the assistance by a number of TNO-FEL personnel: Mr. R. Kemp, M. Roos, J. Nieuwenkamp, M. Moerman and last but not least Mr. P. Fritz. The work for this paper is sponsored by the US Office of Naval Research (ONR grant N00014-94-1-0405).

8. REFERENCES

1. Sadot D., Kitron G., Kitron N., Kopeika N.S.: 1994, Optical Engineering Vol. 33 No. 3, p881: "Thermal imaging through the atmosphere: atmospheric modulation transfer function theory and verification"

2. de Leeuw G., van Eijk A.M.J., Jensen D.R.: 1994, TNO-FEL report FEL-94-A140, "MAPTIP Experiment, Marine Aerosol Properties and Thermal Imager Performance: An overview"

3. de Jong A.N.: 1984, TNO-FEL report PHL 1984-39, "Description of the DUDA scanner"

4. de Jong A.N.: 1977, TNO-FEL report IR 1977-28, "Project Superscan: ETIS II, een scanner met 0,1 mrad resolutie" (text in Dutch)

5. de Jong A.N.: 1978, TNO-FEL report PHL 1978-08, "Long-range transmission measurements over sea water"

6. Davidson K.L., Schafer G.E., Fairall C.W., Goroch A.K.: 1981, Appl. Opt. Vol. 20, 2919-2924, " Verification of the bulk method for calculation overwater optical turbulence"

7. Schwering P.B.W., Kunz, G.: 1995, "Infrared scintillation effects over sea", in "Atmospheric Propagation and Remote Sensing IV", ed. J.C. Dainty, SPIE Vol. 2471, paper-24, Orlando-FL, AeroSense 17-21 April 1995